Hindawi
Journal of Sensors
Volume 2019, Article ID 8498496, 12 pages
https://doi.org/10.1155/2019/8498496

Research Article

A Hybrid Time-Frequency Analysis Method for Railway Rolling-Element Bearing Fault Diagnosis

Yao Cheng, Dong Zou, Weihua Zhang, and Zhiwei Wang

State Key Laboratory of Traction Power, Southwest Jiaotong University, Chengdu 610031, China

Correspondence should be addressed to Dong Zou; zdong_hn@163.com

Received 27 June 2018; Revised 25 September 2018; Accepted 18 October 2018; Published 10 January 2019

Guest Editor: Giuseppe Campobello

The health condition of rolling-element bearings is important for machine performance and operating safety. Due to external interferences, the impulse-related fault information is always buried in the raw vibration signal. To solve this problem, a hybrid time-frequency analysis method combining ensemble local mean decomposition (ELMD) and the Teager-Kaiser energy operator (TKEO) is proposed for the fault diagnosis of high-speed train bearings. The ELMD method is a significant improvement over local mean decomposition (LMD) for addressing the mode-mixing problem. The TKEO method is effective for separating amplitude-modulated (AM) and frequency-modulated (FM) signals from a raw signal. But it is only valid for monocomponent AM-FM signals. The proposed time-frequency method integrates the advantages of ELMD and TKEO to detect localized defects in rolling-element bearings. First, a raw signal is decomposed into an ensemble of PFs and a residual component using ELMD. A novel sensitive parameter (SP) is introduced to select the sensitive PF that contains the most fault-related information. Subsequently, the TKEO is applied to extract both the amplitude and frequency modulations from the selected PF. The experimental results of rolling element and outer race fault signals confirmed that the proposed method could effectively recover fault information from raw signals contaminated by strong noise and other interferences.

1. Introduction

Rolling-element bearing is a critical component of rotating machinery. The malfunction of a rolling-element bearing can cause a decrease in performance or even catastrophic failure with huge economic losses. To monitor the health condition and detect localized defects in a rolling-element bearing, many signal-processing techniques have been proposed and developed in recent years. As one of the most widely-used methods for vibration signal analysis, time-frequency methods, including wavelet transform [1, 2], time-frequency distribution [3, 4], time series model [5, 6], matching pursuit [7, 8], and empirical mode decomposition (EMD) [9], have been explored as powerful tools for fault detection and diagnosis of rolling-element bearings.

Local mean decomposition (LMD), originally proposed by Smith [10] in 2005, is a nonparametric, data-driven time-frequency decomposition method. It adaptively decomposes any complicated multicomponent signal into a series of product functions (PFs), each of which is a product of an envelope signal and a purely frequency-modulated (FM) signal. In addition, the instantaneous amplitude and frequency of each PF can be calculated directly according to the envelope and purely FM signals, respectively. Based on its inherent advantages, LMD is effective for analysing any complicated signal with time-varying frequency, phase, and energy. Most importantly, compared with EMD, the results of LMD are physically plausible, making the conclusions drawn from LMD relevant for various applications. Because of its simple implementation and adequate ability to reveal a signal's nonstationary and nonlinearity information, LMD is widely used as a time-frequency analysis tool for fault diagnosis in rotating machinery [11–15]. However, the mode-mixing phenomenon has a significant influence on the results. It causes LMD to produce different scale oscillations in a single PF or similar scale oscillations in multiple PFs, resulting in some PFs with no physical meaning in the decomposition results. To overcome this drawback of LMD, Yang et al. [16] proposed a noise-assisted time-frequency analysis method called ensemble LMD (ELMD) in 2005.

With ELMD, an ensemble of white noise is added to the original signal, and then the LMD method is used to decompose each of these signals into a series of separate PFs. The final PFs are calculated by averaging the corresponding PFs derived by LMD. The ELMD method can adaptively filter local oscillations into appropriate PFs through the uniform filtering characteristics of white noise, reducing the mode-mixing phenomenon and achieving better decomposition performance compared with LMD. Owing to this significant improvement, ELMD has a diverse range of applications in rotating machinery such as bearing [17, 18] and gear fault diagnoses [19]. However, after performing ELMD on a vibration signal, the added white noise in the raw signal pollutes the PFs and residual signal according to the filter bank structure of LMD. Thus, further procedure is required to precisely and effectively detect the fault characteristic information of rolling-element bearings.

The Teager-Kaiser energy operator (TKEO) was originally proposed by Kaiser in 1990 [20] to measure the energy of a mechanical process, based entirely on the local differential operation without involving any transform. It was designed to extract the amplitude-modulated (AM) and frequency-modulated (FM) signals from a monocomponent AM-FM signal. With its localization property and low computational complexity, the TKEO method has been widely used in machinery fault diagnosis. Liang and Bozchalooi [21] applied the TKEO to extract both the amplitude and frequency modulations of the vibration signals measured from mechanical systems and validated its effectiveness using both simulated and experimental data. Tran et al. [22] proposed a new approach to valve fault diagnosis of reciprocating compressor using three widely used signals involving vibration, pressure, and current of induction motor using TKEO and deep belief networks. Studies on the use of the TKEO technique for signal and image analysis are reviewed herein [23]. It should be noted that TKEO is only valid for monocomponent AM-FM signals. Thus, TKEO always fails to modulate the fault-related information when the analysed signal contains multiple signal components showing modulation phenomenon.

In this paper, a novel hybrid time-frequency analysis method based on ELMD and TKEO is proposed for fault diagnosis in rolling-element bearings. It integrates the merits of ELMD and TKEO to detect localized defects in rolling-element bearings. First, the ELMD method is applied to decompose a multicomponent raw signal measured from faulty rolling-element bearings into a series of PFs, where each PF was a monocomponent AM-FM signal, namely, a product of an envelope signal and a purely FM signal. Second, a sensitive parameter (SP) based on correlated kurtosis (SK) and Pearson's correlation coefficient (PCC) is employed to select the PF component that contains the most characteristic of the fault information. Finally, the TKEO is applied to extract both the amplitude and frequency modulations from the selected PF. Furthermore, the spectrum analysis is used to explore the fault information according to the appearance of the fault characteristic frequencies. To highlight the superiority of the proposed method, some comparisons with two popular signal processing methods including variational mode decomposition [24] and minimum entropy deconvolution (MED) [25, 26] were conducted in the analysis of experimental fault signals.

The rest of this paper is organized as follows. Section 2 briefly introduces the ELMD and TKEO techniques. Section 3 details the proposed hybrid time-frequency analysis method. Section 4 describes the application of the proposed technique to fault diagnosis in rolling elements. Furthermore, comparisons with VMD and MED are conducted in this section. Concluding remarks are presented in Section 5. The introduction should be succinct, with no subheadings. Limited figures may be included only if they are truly introductory and contain no new results.

2. Background Theories

2.1. The Theory of ELMD

2.1.1. LMD. LMD is an adaptive, nonparametric time-frequency analysis method pioneered by Smith [10] in 2005. This method decomposes a raw signal into a series of PFs using the local oscillations of the signal itself. Meanwhile, the instantaneous amplitude and frequency of each PF can be estimated from the corresponding amplitude envelope and FM signals, respectively. The LMD procedure is summarized briefly as follows [10].

Step 1. Find the local extreme points n_i $(i = 1, 2, \dots, M)$ of the targeted signal $x(t)$, where M is the number of extreme points. Then, calculate the local mean value and local envelope magnitude of two successive extreme points as

$$m_i = \frac{n_i + n_{i+1}}{2}, \qquad a_i = \frac{|n_i - n_{i+1}|}{2}. \tag{1}$$

Step 2. Use the moving average algorithm to smooth the local mean values and local amplitudes, and obtain a varying continuous local mean function $m_{1,1}(t)$ and a varying continuous local amplitude function $a_{1,1}(t)$, respectively.

Step 3. Subtract the local mean function from the original signal $x(t)$ and obtain

$$h_{1,1}(t) = x(t) - m_{1,1}(t), \tag{2}$$

where $h_{1,1}(t)$ is the residual signal. Then, $h_{1,1}(t)$ is divided by the amplitude function $a_{1,1}(t)$, resulting in

$$s_{1,1}(t) = \frac{h_{1,1}(t)}{a_{1,1}(t)}. \tag{3}$$

Step 4. Set $s_{1,1}(t)$ as the target signal and repeat steps (1–3) until a purely FM signal $h_{1,n}(t)$ is obtained. This is expressed as

$$\begin{cases} h_{1,1}(t) = x(t) - m_{1,1}(t), \\ h_{1,2}(t) = s_{1,1}(t) - m_{1,2}(t), \\ \qquad \ddots \\ h_{1,n}(t) = s_{1,(n-1)}(t) - m_{1,n}(t), \end{cases} \tag{4}$$

where

$$\begin{cases} s_{1,1}(t) = \dfrac{h_{1,1}(t)}{a_{1,1}(t)}, \\ s_{1,2}(t) = \dfrac{h_{1,2}(t)}{a_{1,2}(t)}, \\ \qquad \ddots \\ s_{1,n}(t) = \dfrac{h_{1,n}(t)}{a_{1,n}(t)}. \end{cases} \tag{5}$$

Step 5. The envelope signal is calculated as

$$a_1(t) = \prod_{i=1}^{n} a_{1,i}(t), \tag{6}$$

and the first PF is given as

$$\mathrm{PF}_1(t) = a_1(t) s_{1,n}(t). \tag{7}$$

The corresponding instantaneous phase $\phi_1(t)$ and instantaneous frequency $f_1(t)$ are calculated as

$$\begin{aligned} \phi_1(t) &= \arccos\left(s_{1,n}(t)\right), \\ f_1(t) &= \frac{f_s d\phi_1(t)}{2\pi dt}. \end{aligned} \tag{8}$$

Step 6. Subtract the derived $\mathrm{PF}_1(t)$ from the original signal $x(t)$, obtaining the signal $u_1(t)$. Then, regard set $u_1(t)$ as the new target signal and repeat the steps (1–5) until $u_J(t)$ is a constant or contains no oscillations:

$$\begin{cases} u_1(t) = x(t) - \mathrm{PF}_1(t), \\ u_2(t) = u_1(t) - \mathrm{PF}_2(t), \\ \qquad \ddots \\ u_J(t) = u_{J-1}(t) - \mathrm{PF}_{J-1}(t). \end{cases} \tag{9}$$

Finally, the original signal can be reconstructed as

$$x(t) = \sum_{j=1}^{J} \mathrm{PF}_j(t) + u_J(t). \tag{10}$$

2.1.2. ELMD. LMD is essentially a filter bank with a self-adaptive bandwidth and centre frequency; however, it is susceptible to mode mixing. The results of LMD often contain pseudo-PFs with no physical meaning, which confuse researchers and engineers in a wide variety of fields. To improve LMD, ELMD was proposed by Yang et al. [16] to mitigate the mode-mixing problem by adding white noise to the original signal. The final ELMD PFs are calculated by taking the ensemble means of the corresponding PFs decomposed from the original signal plus the Gaussian white noise in each trial. A flowchart of the ELMD algorithm is illustrated in Figure 1:

Step 1. For any trial index $i\,(i = 1, 2, \ldots, I)$, add the white noise $\beta n_i(t)$ to the original signal $x(t)$ to generate the polluted signal $x_i(t)$:

$$x_i(t) = x(t) + \beta n_i(t), \tag{11}$$

where $n_i(t)$ denotes the white noise with zero mean and unit variance, β is the amplitude of the added white noise, and I is the trial number.

Step 2. Decompose the polluted signal $x_i(t)$ using the LMD algorithm:

$$x_i(t) = \sum_{j=1}^{J} \mathrm{PF}_{i,j}(t) + u_i(t), \tag{12}$$

where $\mathrm{PF}_{i,j}(t)$ is the jth PF of the ith trial, $u_i(t)$ denotes the residual of the ith trial, and J is the number of PFs.

Step 3. Calculate the ensemble means of the corresponding decomposed PFs:

$$\mathrm{PF}_j(t) = \frac{1}{I} \sum_{j=1}^{I} \mathrm{PF}_{i,j}(t), \tag{13}$$

where $\mathrm{PF}_j(t)$ is the jth PF for $j = 1, 2, \ldots, J$.

2.2. The Theory of TKEO. The Teager-Kaiser energy operator (TKEO) is an attractive demodulation method proposed by Kaiser [20]. It is an alternative for obtaining the amplitude-modulated (AM) signal and frequency-modulated (FM) signal from the vibration signal. For a continuous time signal $x(t)$, the TKEO is defined as

$$\psi[x(t)] = \left(\frac{dx(t)}{dt}\right)^2 - x(t)\frac{d^2x(t)}{dt^2}. \tag{14}$$

Thus, the TKEO is defined in discrete format by [21]

$$\psi[x(n)] = [x(n)]^2 - x(n+1)x(n-1). \tag{15}$$

As a signal demodulation method, TKEO offers superior performance in recovering the time-frequency information of a vibration signal and provides a vital approach for fault diagnosis of rolling-element bearings. Note that the TKEO method is only applicable to monocomponent AM-FM signals. This shortcoming greatly limits the wide application of TKEO. For a multicomponent signal, a decomposition or

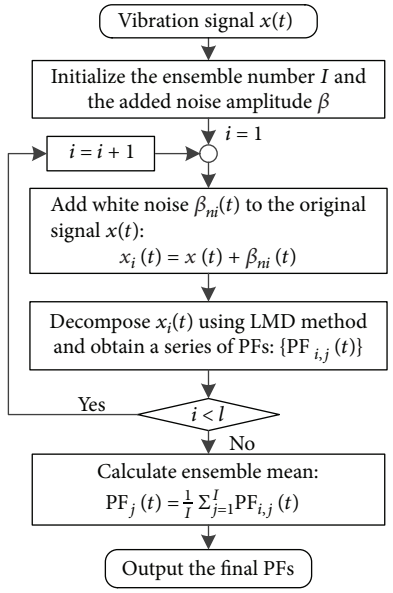

Figure 1: The flowchart of the ELMD method.

modulated procedure is always necessary before the implementation of TKEO.

3. Time-Frequency Analysis Method Based on ELMD and TKEO

3.1. Selection of Sensitive PF. The ELMD method can yield better decomposition performance than the classical LMD method in terms of overcoming the mode-mixing problem and reducing the pseudo modes. However, the existing noise still remains in the PFs according to the filter bank structure of LMD. Thus, to achieve a precise fault detection result, it is necessary to carefully select the PF component. Most of the studies conducted so far ignored systematic selection of most effective PFs for bearing diagnosis. Kurtosis is sensitive to the impacts induced by localized defects and thus is widely chosen to select the sensitive PF containing the most fault-related information. But it is also sensitive to random impulses caused by external interferences on the bearing housing. Correlated kurtosis [24] is another index for measuring the intensity of periodic impulses. The first-shift correlated kurtosis of the jth PF is defined as follows:

$$\mathrm{CK}_j = \frac{\sum_{n=1}^{N}\left(\mathrm{PF}_j(n)\mathrm{PF}_j(n-mT)\right)^2}{\left(\sum_{n=1}^{N}\mathrm{PF}_j{}^2(n)\right)^2}, \tag{16}$$

where T is the fault period of interest and is calculated as follows:

$$T = \frac{\mathrm{Fs}}{f_m}, \tag{17}$$

where f_m and Fs are the fault frequency and the sampling frequency, respectively. When the fault period T, calculated according to Equation (17), is a fractional number, the resampling technique is necessary before the iterative procedure can be implemented [26]. Compared to kurtosis, correlated kurtosis remains unaffected by the random impulses and is more robust and more suitable for detecting the fault-related information contained in PFs.

Besides, Pearson's correlation coefficient (PCC) is widely used to select the sensitive PF. It measures the consistence between the recovered signal and the reference signal. The $PCC_j(j = 1, 2, \ldots, J)$ between the jth PF of the raw signal $x(n)$ and the raw signal $x(n)$ is defined as

$$\mathrm{PCC}_j = \frac{(\mathbf{x} - \bar{\mathbf{x}})^T\left(\mathrm{PF}_j - \bar{\mathrm{PF}}_j\right)}{\|\mathbf{x} - \bar{\mathbf{x}}\| \cdot \left\|\mathrm{PF}_j - \bar{\mathrm{PF}}_j\right\|}, \tag{18}$$

where $\|\cdot\|$ represents the root-mean-square operator and $\bar{\mathbf{x}}$ and $\bar{\mathrm{PF}}_j$ represent the mean values of $\mathbf{x}$ and PF_j, respectively. Note that the value of PCC_j is limited in [0, 1]. The sensitive parameter (SP) of the jth PF is defined as

$$\mathrm{SP}_j = \mathrm{PCC}_j \cdot f_j, \tag{19}$$

where

$$f_j = \frac{\mathrm{CK}_j - \min(\mathrm{CK})}{\max(\mathrm{CK}) - \min(\mathrm{CK})}. \tag{20}$$

To avoid extreme value of CK, the min–max normalization technique is utilized to normalizing the function f_j ranging from 0 to 1. Hence, after calculating using Equation (20), the PF with maximum correlation value will be normalized to a value of 1 and the PF with the least correlation is normalized to a value of 0. Only the first 6 PFs from the decomposition are considered in this study as the remaining PFs are typically residual or trends and do not contain bearing-related fault information.

3.2. Time-Frequency Analysis Method for Fault Detection of Rolling-Element Bearings. A novel time-frequency method combing the capabilities of ELMD and TKEO, automatically decomposing a nonstationary signal into PFs and extracting the AM signal, respectively, is proposed for fault detection and diagnosis of rolling-element bearings. In the proposed method, a series of PFs is obtained using ELMD and the PF that contains the most fault-related information is selected according to the SP value. Then, the TKEO method is adopted to obtain the amplitude and frequency modulations from the selected PF. The scheme of the proposed method for fault diagnosis of rolling-element bearings is illustrated in Figure 2.

Step 1. Decompose original vibration signal into a series of PFs using ELMD.

Step 2. Calculate the SP value of each PF, and select a sensitive PF based on the SP value.

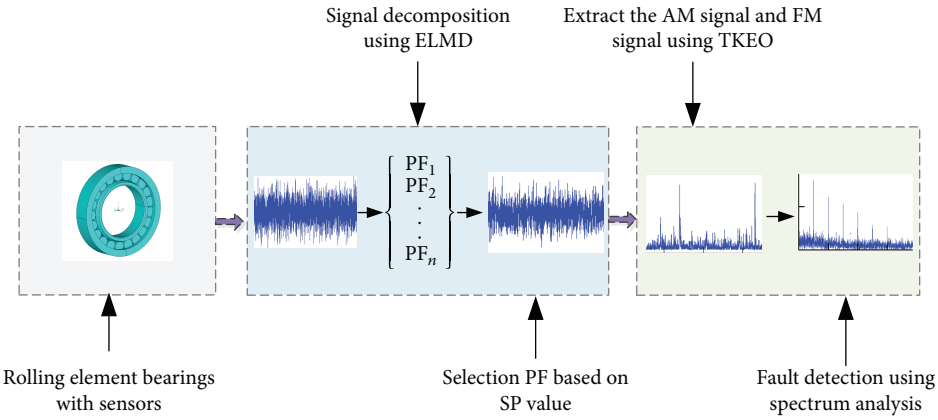

Figure 2: Flowchart of the proposed method.

Step 3. Extract the amplitude and frequency modulations from the selected PF using TKEO.

Step 4. Detect faults using spectrum analysis.

4. Experiment Results

To demonstrate the effectiveness of the proposed time-frequency analysis method, high-speed train bearing fault signals measured in a bearing test rig are analysed in this section. The experimental test rig and the investigated faulty bearing are presented in Figure 3. Two accelerometer sensors mounted on the shaft box were used to collect vibration signals from the faulty bearings. The defects on the rolling element and outer race were implanted artificially with a width of 0.2 mm and a depth of 0.3 mm. The rolling element number (n), rolling element diameter (d), rolling element pitch diameter (D), and load angle (ϕ) were 17, 26.691 mm, 187.205 mm, and 12.083 degree, respectively. The four types of bearing characteristic frequency, namely, bearing pass frequency of outer race (BPFO), bearing pass frequency of inner race (BPFI), ball spin frequency (BSF), and fundamental train frequency (FTF), can be calculated as follows [27]:

$$\begin{aligned}
\mathrm{BPFO} &= \frac{nf_r}{2}\left(1 - \frac{d}{D}\cos\phi\right),\\
\mathrm{BPFI} &= \frac{nf_r}{2}\left(1 + \frac{d}{D}\cos\phi\right),\\
\mathrm{BSF} &= \frac{D}{2d}\left[1 - \left(\frac{d}{D}\cos\phi\right)^2\right],\\
\mathrm{FTF} &= \frac{f_r}{2}\left(1 - \frac{d}{D}\cos\phi\right),
\end{aligned} \tag{21}$$

where f_r is the shaft speed. The sampling frequency and signal length were 5120 Hz and 8192, respectively. In addition, in the experimental analysis, the amplitude of the added white noise β and the trial number I of the ELMD were set as 0.1 and 100, respectively.

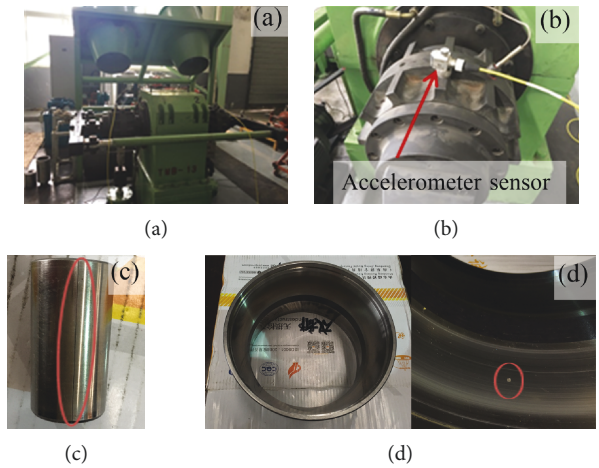

Figure 3: Experimental equipment and faulty elements of the tested high-speed train bearings: (a) test rig; (b) location of accelerometer sensor; (c) localized defect on rolling element; (d) localized defect on outer race.

4.1. Bearing with a Rolling Element Fault at Rotation Speed of 818 rpm. The rolling element fault signal was measured at a shaft rotational speed of 818 rpm, and the fault characteristic frequency BSF and rotational frequency were 46.9 Hz and 13.6 Hz, respectively. Figure 4 presents the fault signal of rolling element and its envelope spectrum, respectively. The BSF and its harmonics are completely buried in the envelope spectrum, and no useful information can be identified to detect the localized defect on the rolling element, as shown in Figure 4(b).

Figure 5 displays the decomposition results of the rolling element signal obtained using ELMD. The raw signal is decomposed into seven PFs and one residual component. SP is employed to quantify the impulse amplitude of each PF, as illustrated in Table 1. The first PF has the largest SP value, indicating that it contains the most fault-related information. Figures 6(a) and 6(b) display the resulting signal of the selected PF_1 obtained using TKEO, along with the corresponding TKEO spectrum. It should be noted that the characteristic frequency BSF and its first three harmonics can be

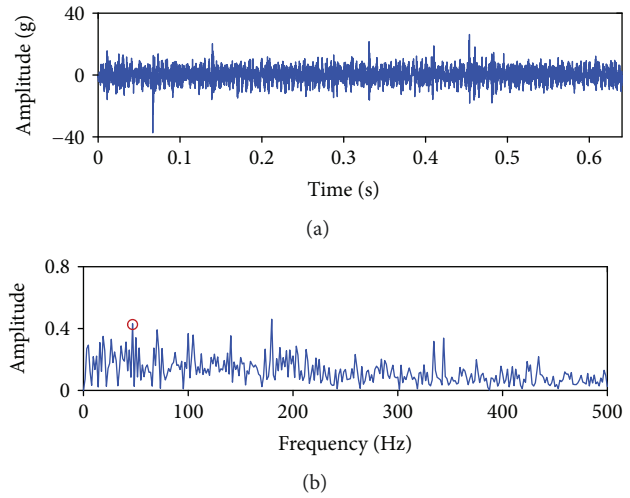

Figure 4: Rolling element fault signal and its envelope spectrum: (a) raw signal; (b) envelope spectrum.

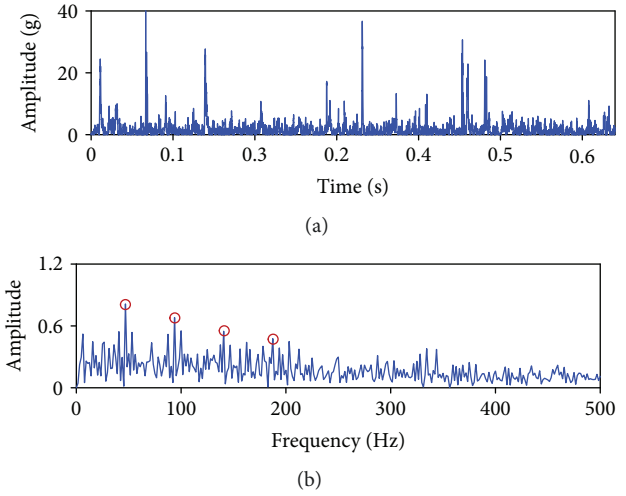

Figure 6: Results of the selected PF1 obtained using TKEO: (a) time-domain signal; (b) TKEO spectrum.

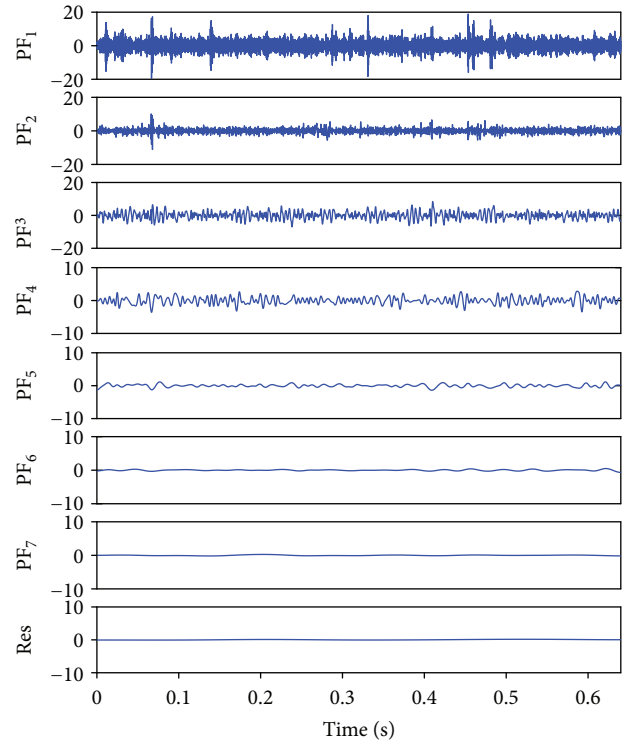

Figure 5: Decomposition results of the rolling element fault signal obtained using ELMD.

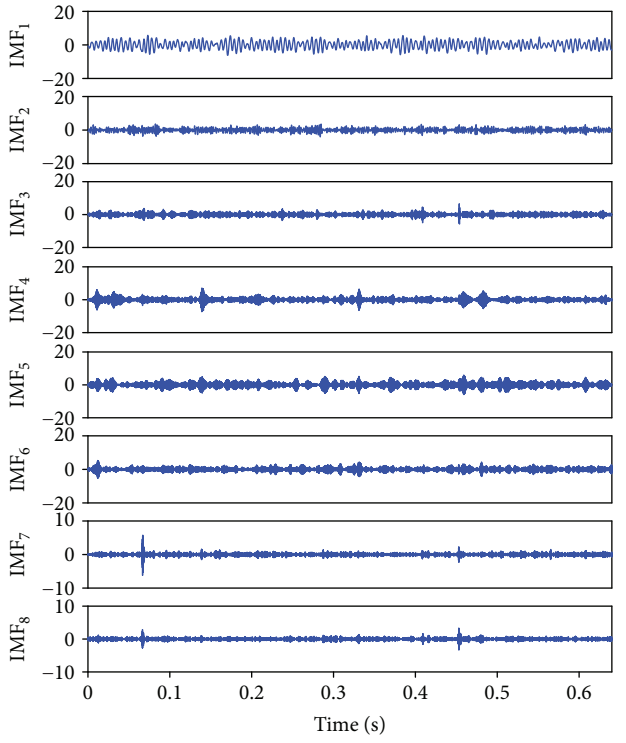

Figure 7: Decomposition results of the rolling element fault signal obtained using VMD.

Table 1: SP values of the first six PFs obtained using ELMD.

Mode	PF_1	PF_2	PF_3	PF_4	PF_5	PF_6
SP	0.4182	0.1152	0.1289	0.0764	0	0.0185

clearly identified from the TKEO spectrum of the selected PF_1, which immediately indicates a localized defect on the rolling element.

To further validate the effectiveness of the proposed method, VMD [24] and MED [25, 26] are utilized to compare with the proposed method by processing the rolling-element bearing fault signal. VMD is a newly proposed time-frequency analysis method, and a nonrecursion decomposition procedure is designed to decompose the multicomponent signal into several finite bandwidth single components (IMF) with sparse features. MED is a classical deconvolution method for recovering the fault-related impulses from the

Table 2: SP values of IMFs obtained using VMD.

Mode	IMF1	IMF2	IMF3	IMF4	IMF5	IMF6	IMF7	IMF8
SP	0.1017	0.0544	0	0.4228	0.2076	0.0227	0.0785	0.0480

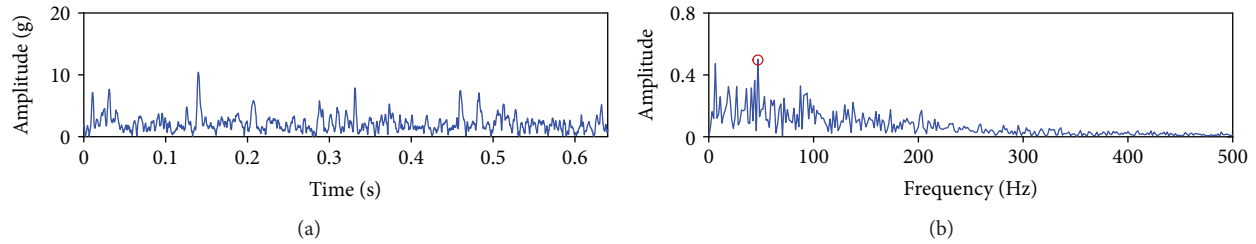

Figure 8: Results of the selected IMF5 obtained using VMD: (a) envelope signal; (b) envelope spectrum.

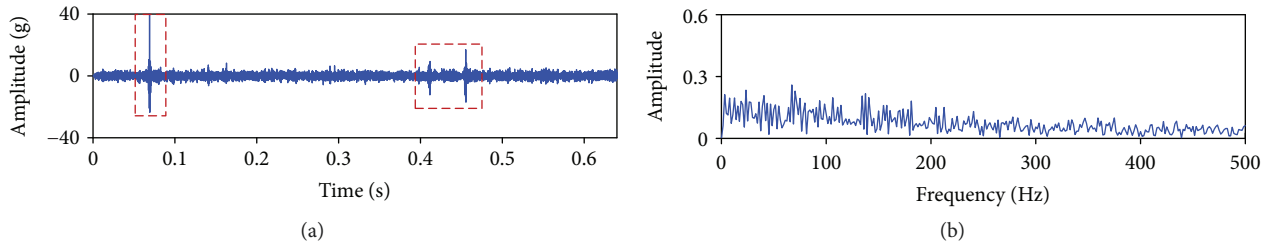

Figure 9: Results of MED: (a) filtered signal; (b) envelope spectrum of the filtered signal.

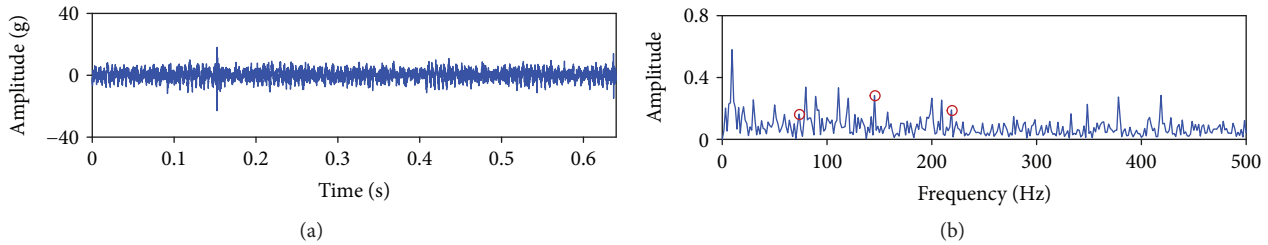

Figure 10: Outer race fault signal and its envelope spectrum: (a) raw signal; (b) envelope spectrum.

raw vibration signal. The inverse filter of MED is iteratively solved by maximizing the kurtosis of the filtered signal. Figure 7 shows the decomposition results of VMD by setting the number of the IMFs as 8. According to the SP value of each IMF as listed in Table 2, the fourth IMF is selected as the sensitive signal component to further identify the fault information. Figure 8 displays the envelope signal and envelope spectrum of the selected IMF4, respectively. It shows that only the fault frequency can be found and its harmonics are submersed in the envelope spectrum, as displayed in Figure 8(b). The results of MED are presented in Figure 9. The filter length and number of iterations are 40 and 100, respectively. It shows that the large impulses have great influence on the performance of MED, as shown in Figure 9(a), and the envelope spectrum of the filtered signal provides no information about the localized defect on the rolling element. In conclusion, the proposed method has better performance in comparison with VMD and MED in this case study.

4.2. Bearing with an Outer Race Fault at Rotation Speed of 602 rpm. The outer race fault signal measured at a rotation speed of 602 rpm further validated the effectiveness of the proposed method. The fault characteristic frequency PBFO is 73.4 Hz. The raw outer race fault signal and its envelope spectrum are plotted in Figure 10, respectively. Note that the envelope spectrum is dominated by the interference frequencies. Seven PFs and one residual signal decomposed by ELMD are presented in Figure 11. Table 3 lists the SP values of the first six PFs, from which the first PF is selected. Figures 12(a) and 12(b) show the resultant signal of the selected PF_1 obtained using TKEO and the corresponding

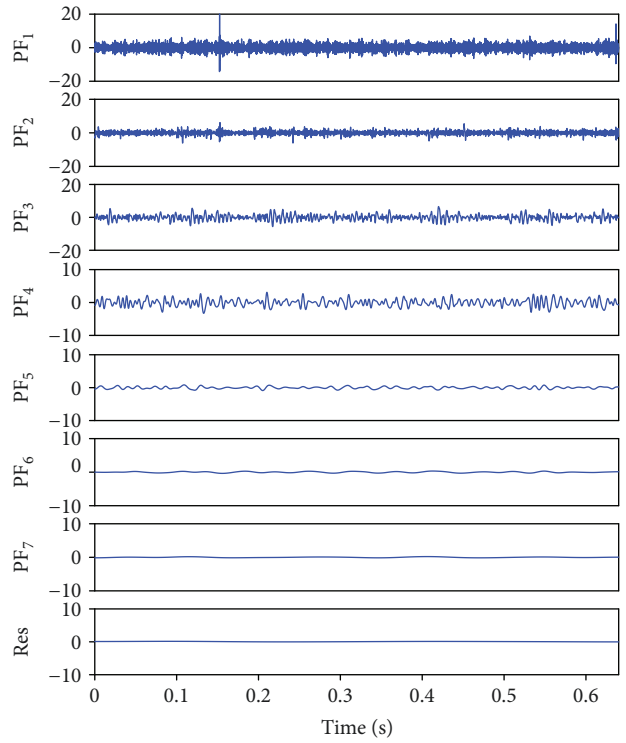

Figure 11: Decomposition results of the outer race fault signal obtained using ELMD.

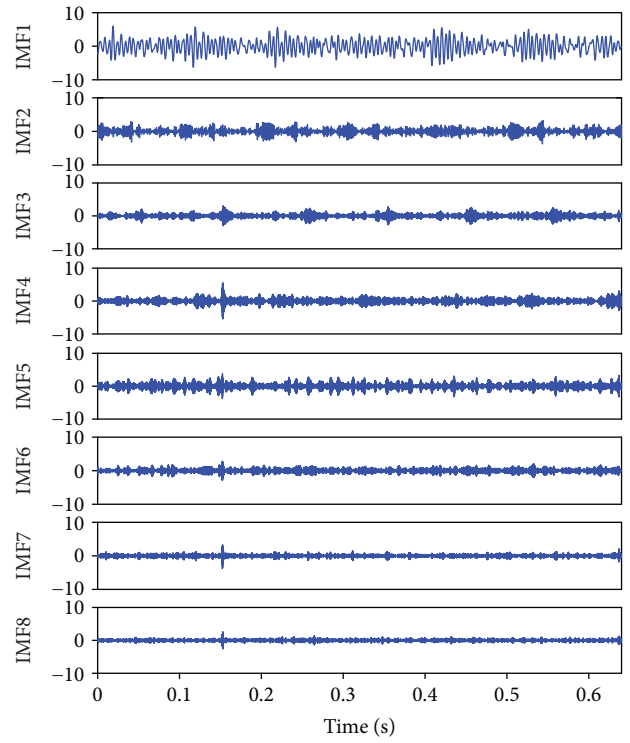

Figure 13: Decomposition results of the rolling element fault signal obtained using VMD.

Table 3: SP values of the first six PFs obtained using ELMD.

Mode	PF_1	PF_2	PF_3	PF_4	PF_5	PF_6
SP	0.4403	0.1914	0.0538	0.1725	0.0873	0

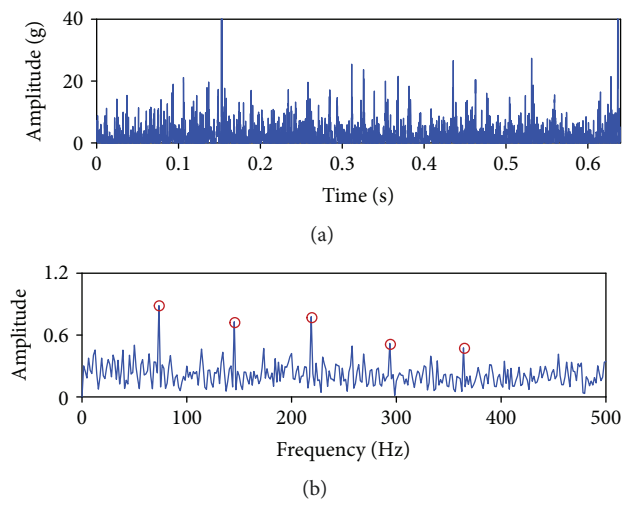

Figure 12: Results of the selected PF_1 obtained using TKEO: (a) time-domain signal; (b) TKEO spectrum.

TKEO spectrum, respectively. The BPFO (73.4 Hz) and its first four harmonics are easily identified in the TKEO spectrum of the selected PF_1, as shown in Figure 12(b), indicating the effectiveness of the proposed time-frequency method in this analysis.

Figure 13 presents the IMF components of VMD, and Table 4 lists the SP of each IMF shown in Figure 13. The fifth PF has the largest SP value, indicating that it contains the most fault-related information. The envelope signal of IMF5 and the responding envelope spectrum are displayed in Figure 14, respectively. It shows that only the amplitude of BPFO, 2BPFO, and 3BPFO can be easily identified from the envelope spectrum and the amplitudes of 4BPFO and 5BPFO are mixed, as shown in Figure 14(b). Figure 15 presents the results obtained by MED. It shows that the MED prefers to deconvolve a single impulse, and only the amplitudes of 2BPFO and 3BPFO can be found in the envelope spectrum of the filtered signal, as shown in Figure 15(b). Again, the proposed method outperforms VMD and MED.

4.3. Bearing with an Outer Race Fault at Rotation Speed of 884 rpm. In the last experimental case, we analyse the outer race fault signal measured at a rotation speed of 884 rpm. The bearing pass frequency of the outer race (BPFO) is 107.9 Hz. The measured outer race fault signal and its envelope spectrum are plotted in Figure 16. It shows that, because of the existing strong noise, the BPFO amplitudes and its harmonics are buried in the envelope spectrum of the raw vibration signal. Figure 17 displays the decomposition results of the raw signal obtained using ELMD. It shows that the raw signal is decomposed into eight PFs and one residual component. According to the SP values listed in Table 5, the first PF

Table 4: SP values of IMFs obtained using VMD.

Mode	IMF1	IMF2	IMF3	IMF4	IMF5	IMF6	IMF7	IMF8
SP	0.121	0	0.0902	0.1205	0.3514	0.1388	0.1422	0.0500

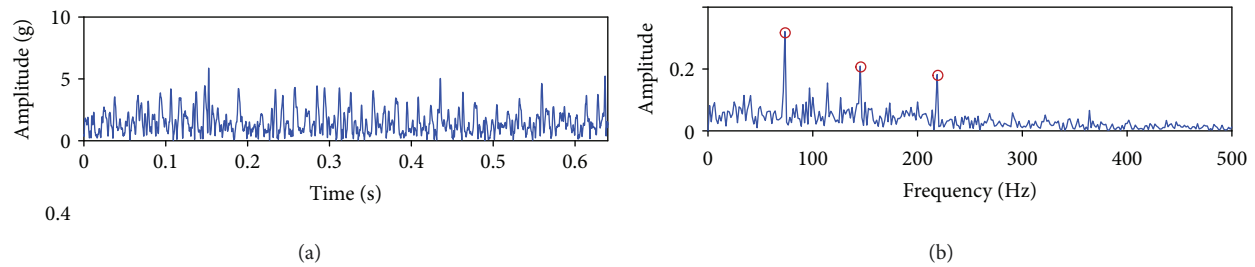

Figure 14: Results of the selected IMF5 obtained using VMD: (a) envelope signal; (b) envelope spectrum.

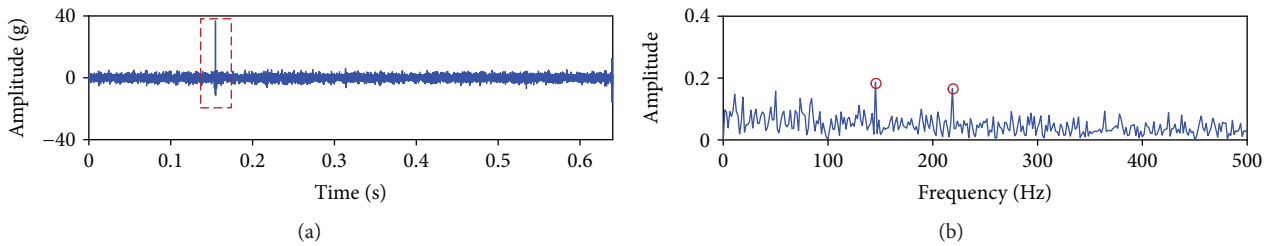

Figure 15: Results of MED: (a) filtered signal; (b) envelope spectrum of the filtered signal.

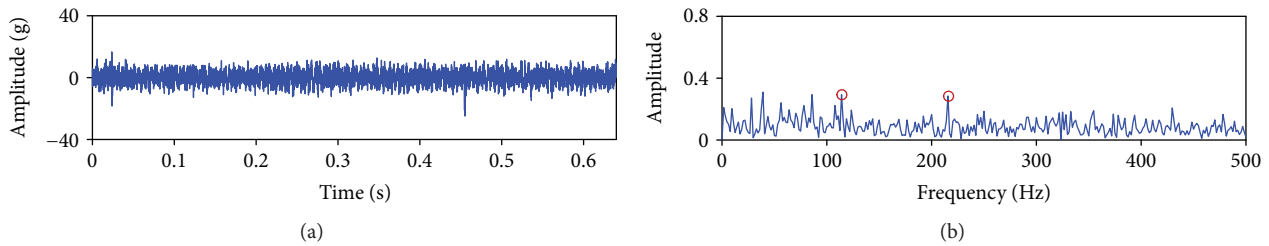

Figure 16: Outer race fault signal and its envelope spectrum: (a) raw signal; (b) envelope spectrum.

is selected as the sensitive signal. Figures 18(a) and 18(b) display the resulting signal of the selected PF_1 obtained using TKEO, along with the corresponding TKEO spectrum. The characteristic frequency of BPFO and its first harmonic (2BPFO) can be easily recognized from the envelope spectrum shown in Figure 18(b). In conclusion, this case study confirms the effectiveness of the proposed hybrid time-frequency method.

Appling VMD to decompose the outer race fault signal, the results are presented in Figure 19. Table 6 lists the SP values of the IMF components, and the sixth IMF is selected as the sensitive signal component. Figure 20 displays the envelope signal and envelope spectrum of IMF6 obtained by VMD, respectively. The amplitudes of BPFO and 2BPFO are noticeable in the envelope spectrum shown in Figure 20(b). However, the amplitudes of the BPFO and 2BPFO are notably larger in the envelope spectrum obtained by the proposed method (Figure 18(b)) than in that determined by VMD (Figure 20(b)), indicating the superiority of the proposed method over the VMD in this case. The results obtained by MED are presented in Figure 21. Again, the deconvolution method fails to deconvolve the fault-related signal component and the envelope spectrum of the filtered signal contained on fault information.

5. Conclusions

In this paper, a hybrid time-frequency analysis method based on ELMD and TKEO was proposed for the fault diagnosis of rolling-element bearings. The ELMD method, as an

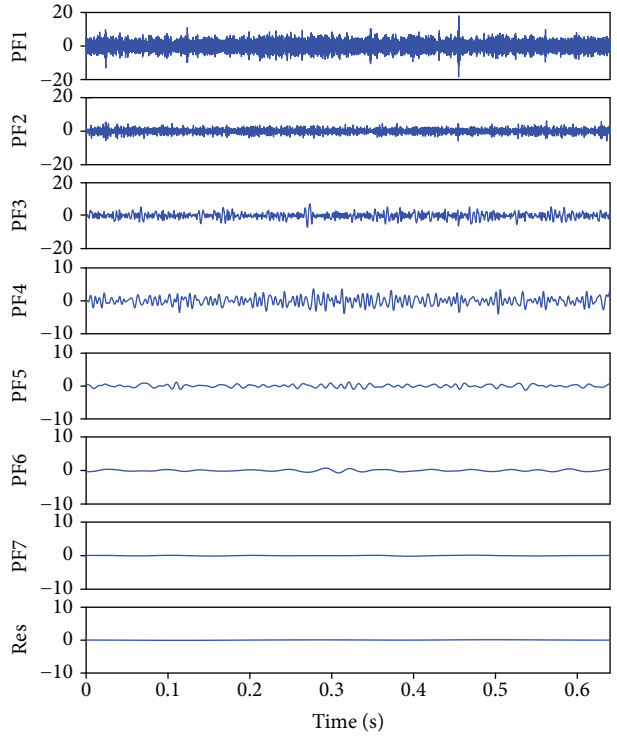

Figure 17: Decomposition results of the outer race fault signal obtained using ELMD.

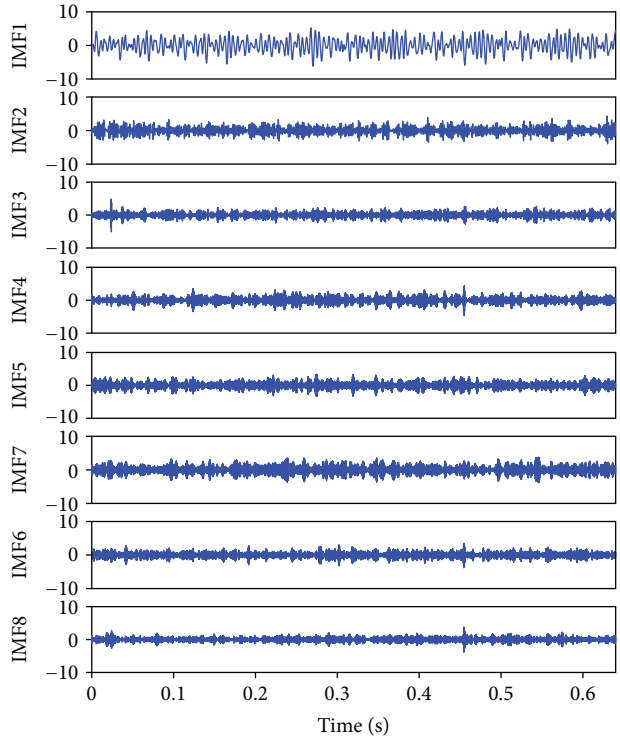

Figure 19: Decomposition results of the rolling element fault signal obtained using VMD.

Table 5: SP values of the first six PFs obtained using ELMD.

Mode	PF_1	PF_2	PF_3	PF_4	PF_5	PF_6
SP	0.3800	0.1623	0	0.1000	0.1104	0.0113

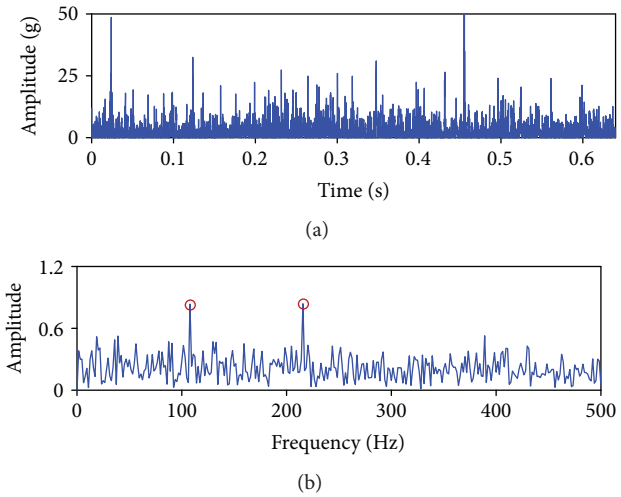

Figure 18: Results of the selected PF1 obtained using TKEO: (a) time-domain signal; (b) TKEO spectrum.

improved version of the original LMD, can effectively alleviate the mode-mixing phenomenon by adding an ensemble of Gaussian white noise to the raw signal. The TKEO method is a powerful tool for extracting the AM and FM signals from a monocomponent AM-FM signal and is well adapted for enhancing the fault information of rotation machinery. The proposed time-frequency analysis method integrates the merits of ELMD and TKEO and involves two steps. First, the raw signal is decomposed into a series of PFs by using ELMD, and the PF that contains the most fault-related information is selected based on the SP value. Subsequently, TKEO is applied to extract the fault signal contained in the selected sensitive PF. The rolling element and the outer race fault signals were investigated to verify the effectiveness of the proposed time-frequency method. The experimental results confirmed that the proposed method could effectively recover the fault information from a raw signal contaminated with strong noise and other interferences. The comparison analysis with VMD and MED further confirmed the superiority of the proposed method.

The next step of this research will shift toward applying the proposed method to the fault diagnosis of other rotating machinery, such as gearing and motor. Furthermore, with the rapid development in the hardware and fault detection technology, the proposed method can compare with an increasing number of state-of-the-art techniques.

Data Availability

The data used to support the findings of this study are available from the corresponding author upon request.

Table 6: SP values of IMFs obtained using VMD.

Mode	IMF1	IMF2	IMF3	IMF4	IMF5	IMF6	IMF7	IMF8
SP	0.0844	0	0.2443	0.3130	0.2680	0.3670	0.2174	0.2441

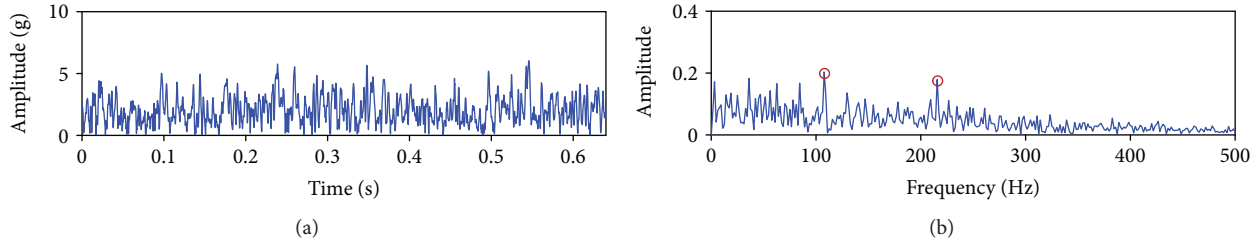

Figure 20: Results of the selected IMF5 obtained using VMD: (a) envelope signal; (b) envelope spectrum.

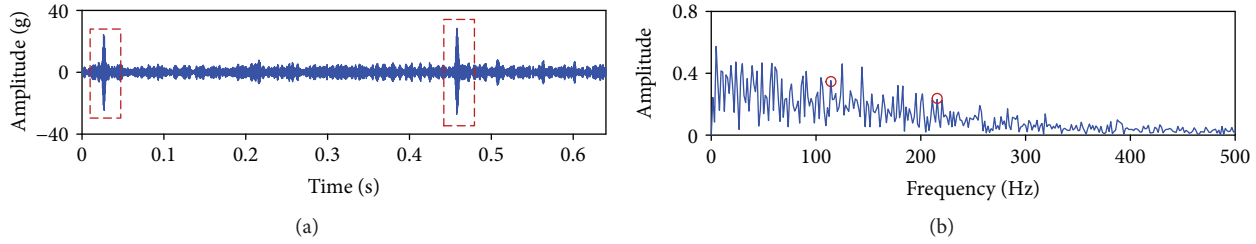

Figure 21: Results of MED: (a) filtered signal; (b) envelope spectrum of the filtered signal.

Disclosure

An earlier version of the manuscript 8498496 presented in ICPHM 2018 has been removed (the paper was not presented at this conference).

Conflicts of Interest

The authors declare that there is no conflict of interest regarding the publication of this paper.

Authors' Contributions

Yao Cheng contributed significantly to analysis and manuscript preparation. Dong Zou contributed to the conception of the study. Weihua Zhang helped perform the analysis with constructive discussions. Zhiwei Wang performed the data analyses and wrote the manuscript.

Acknowledgments

This project is supported by China Railway Corporation Technology Research and Development Program (2017J008-L), National Natural Science Foundation of China (no. 51475391), Fundamental Research Funds for the Central Universities (2682018CX71), and National Key Research and Development Program of China (no. 2016YFB1200506-02), which are highly appreciated by the authors. The authors would also thank supports from State Key Laboratory of Traction Power, Southwest Jiaotong University (no. 2015TPL_T03).

References

[1] S. Prabhakar, A. R. Mohanty, and A. S. Sekhar, "Application of discrete wavelet transform for detection of ball bearing race faults," *Tribology International*, vol. 35, no. 12, pp. 793–800, 2002.

[2] D. Paliwal, A. Choudhury, and G. Tingarikar, "Wavelet and scalar indicator based fault assessment approach for rolling element bearings," *Procedia Materials Science*, vol. 5, pp. 2347–2355, 2014.

[3] A. H. Costa and S. Hengstler, "Adaptive time–frequency analysis based on autoregressive modeling," *Signal Processing*, vol. 91, no. 4, pp. 740–749, 2011.

[4] D. Onchis, "Observing damaged beams through their time-frequency extended signatures," *Signal Processing*, vol. 96, pp. 16–20, 2014.

[5] D. C. Baillie and J. Mathew, "A comparison of autoregressive modeling techniques for fault diagnosis of rolling element bearings," *Mechanical Systems and Signal Processing*, vol. 10, no. 1, pp. 1–17, 1996.

[6] J. Ma, F. Xu, K. Huang, and R. Huang, "GNAR-GARCH model and its application in feature extraction for rolling bearing fault diagnosis," *Mechanical Systems & Signal Processing*, vol. 93, no. 1, pp. 175–203, 2017.

[7] J. Wang, J. Zhang, C. Chen, F. Tian, and L. Cui, "Basic pursuit of an adaptive impulse dictionary for bearing fault diagnosis,"

in *2014 International Conference on Mechatronics and Control (ICMC)*, pp. 2840–2862, Jinzhou, China, July 2014.

[8] L. Cui, N. Wu, C. Ma, and H. Wang, "Quantitative fault analysis of roller bearings based on a novel matching pursuit method with a new step-impulse dictionary," *Mechanical Systems & Signal Processing*, vol. 68-69, pp. 34–43, 2016.

[9] N. E. Huang, Z. Shen, S. R. Long et al., "The empirical mode decomposition and the Hilbert spectrum for nonlinear and non-stationary time series analysis," *Proceedings of the Royal Society A: Mathematical, Physical and Engineering Sciences*, vol. 454, no. 1971, pp. 903–995, 1998.

[10] J. S. Smith, "The local mean decomposition and its application to EEG perception data," *Journal of the Royal Society Interface*, vol. 2, no. 5, pp. 443–454, 2005.

[11] Y. Wang, Z. He, and Y. Zi, "A demodulation method based on improved local mean decomposition and its application in rub-impact fault diagnosis," *Measurement Science and Technology*, vol. 20, no. 2, article 025704, 2009.

[12] Y. Wang, Z. He, and Y. Zi, "A comparative study on the local mean decomposition and empirical mode decomposition and their applications to rotating machinery health diagnosis," *Journal of Vibration and Acoustics*, vol. 132, no. 2, pp. 613–624, 2010.

[13] C. Park, D. Looney, M. M. van Hulle, and D. P. Mandic, "The complex local mean decomposition," *Neurocomputing*, vol. 74, no. 6, pp. 867–875, 2011.

[14] Y. Wang, Z. He, J. Xiang, and Y. Zi, "Application of local mean decomposition to the surveillance and diagnostics of low-speed helical gearbox," *Mechanism & Machine Theory*, vol. 47, no. 1, pp. 62–73, 2012.

[15] Z. Liu, Y. Jin, M. J. Zuo et al., "Time-frequency representation based on robust local mean decomposition for multicomponent AM-FM signal analysis," *Mechanical Systems and Signal Processing*, vol. 95, pp. 468–487, 2016.

[16] Y. Yang, J. Cheng, and K. Zhang, "An ensemble local means decomposition method and its application to local rub-impact fault diagnosis of the rotor systems," *Measurement*, vol. 45, no. 3, pp. 561–570, 2012.

[17] Z. Liu, M. J. Zuo, Y. Jin, D. Pan, and Y. Qin, "Improved local mean decomposition for modulation information mining and its application to machinery fault diagnosis," *Journal of Sound and Vibration*, vol. 397, pp. 266–281, 2017.

[18] L. Wang, Z. Liu, Q. Miao, and X. Zhang, "Time-frequency analysis based on ensemble local mean decomposition and fast kurtogram for rotating machinery fault diagnosis," *Mechanical Systems and Signal Processing*, vol. 103, pp. 60–75, 2018.

[19] C. Zhang, Z. Li, C. Hu, S. Chen, J. Wang, and X. Zhang, "An optimized ensemble local mean decomposition method for fault detection of mechanical components," *Measurement Science & Technology*, vol. 28, no. 3, article 035102, 2017.

[20] J. F. Kaiser, "On a simple algorithm to calculate the 'energy' of a signal," in *International Conference on Acoustics, Speech, and Signal Processing*, pp. 381–384, Albuquerque, NM, USA, April 2002.

[21] M. Liang and I. S. Bozchalooi, "An energy operator approach to joint application of amplitude and frequency-demodulations for bearing fault detection," *Mechanical Systems and Signal Processing*, vol. 24, no. 5, pp. 1473–1494, 2010.

[22] V. T. Tran, F. Althobiani, and A. Ball, "An approach to fault diagnosis of reciprocating compressor valves using Teager–Kaiser energy operator and deep belief networks," *Expert Systems with Applications*, vol. 41, no. 9, pp. 4113–4122, 2014.

[23] A. O. Boudraa and F. Salzenstein, "Teager–Kaiser energy methods for signal and image analysis: a review," *Digital Signal Processing*, vol. 78, pp. 338–375, 2018.

[24] K. Dragomiretskiy and D. Zosso, "Variational mode decomposition," *IEEE Transactions on Signal Processing*, vol. 62, no. 3, pp. 531–544, 2014.

[25] C. A. Cabrelli, "Minimum entropy deconvolution and simplicity: a noniterative algorithm," *Geophysics*, vol. 50, no. 3, pp. 394–413, 2012.

[26] G. L. Mcdonald, Q. Zhao, and M. J. Zuo, "Maximum correlated kurtosis deconvolution and application on gear tooth chip fault detection," *Mechanical Systems and Signal Processing*, vol. 33, no. 1, pp. 237–255, 2012.

[27] A. Rai and S. H. Upadhyay, "A review on signal processing techniques utilized in the fault diagnosis of rolling element bearings," *Tribology International*, vol. 96, pp. 289–306, 2016.